http://mmg.tversu.ru ISSN 2311-1275

Mathematical Modelling and Geometry

Volume 12, No 1, pp. 1 – 18 (2024) doi:10.26456/mmg/2024-1211

Discrete Dynamics of State Parameters of Fractal Thermodynamics of Covid-19 Pandemics

V. P. Tsvetkov[1,a], **S. A. Mikheev**[1,b], **I. V. Tsvetkov**[1,c], **V. L. Derbov**[2,d], **A. A. Gusev**[3,e], **S. I. Vinitsky**[3,4,f]

[1] Tver State University, 33, Zhelyabova St., Tver 170100 Russia
[2] N. G. Chernyshevsky Saratov National Research State University, Saratov, Russia
[3] Joint Institute for Nuclear Research, Dubna, Russia
[4] Peoples' Friendship University of Russia (RUDN), 117198 Moscow, Russia

e-mail: [a] Tsvetkov.VP@tversu.ru
ORCID: [a] 0000-0001-8842-8076 [b] 0000-0001-7749-6460 [c] 0000-0002-5284-880X
[d] 0000-0001-5450-3963 [e] 0000-0003-4897-6128 [f] 0000-0003-3078-0047

Received 8 April 2024, in final form 25 April. Published 28 April 2024.

Abstract. ***Background:*** Currently, one of the urgent tasks of mathematical modeling is the construction of mathematical models that adequately describe pandemics, in particular, the Covid-19 pandemic. In recent few years, many studies have been devoted to solving this problem, using various methods and approaches. Purpose: The paper reveals the characteristic features of the discrete dynamics of state parameters in the fractal thermodynamics of Covid-19 pandemic from 01/22/2020 to 09/21/2022. These features are shown to be useful for forecasting discrete dynamics of pandemics and analogous processes.
Methods: In recent few years, many studies have been devoted to solving this problem, using various methods and approaches. In most of these studies, the raw data is the number of daily diseases $\nu(t)$ determined from the approved statistical data. A fundamentally new approach to the study of $\nu(t)$ is implies the use of fractal and multifractal analysis.
Results: If we approximate the set of all states (S_{f_i}, T_{f_i}) by fractal state equations $S_f = AT_f^{\gamma}$, then this set turns out to divide into subsets, each most close to a certain fractal equation of state, determined by parameter γ and A. This gives rise to a discrete dynamics of fractal phase states, determined by the jumps in the parameters γ and A. A passage to the limit yields the following asymptotic fractal equation of state: $S_f = 12.143T_f^{0.0147}$. It is shown that the jumps in the parameters A, γ lead to fractal phase transitions between fractal phase states of Covid-19 pandemics. An analytic continuation to the forecast period yields the values of forecast coefficients $A_{IV} = 11.7580, \gamma_{IV} = 0.01475$.
Conclusions: In this paper the characteristic features of the discrete dynamics of the fractal thermodynamic state parameters of the Covid-19 pandemic from 01/22/2020 to 09/21/2022 are revealed. It is shown that these features can be used to predict the discrete dynamics of pandemics and other similar processes.

Keywords: mathematical model, fractal thermodynamics, Covid-19 pandemic, dominating variant of Covid-19, discrete dynamics

1. Introduction

Currently, one of the urgent tasks of mathematical modeling is the construction of mathematical models that adequately describe pandemics, in particular, the Covid-19 pandemic. In recent few years, many studies have been devoted to solving this problem [1–15], using various methods and approaches. In most of these studies, the raw data is the number of daily diseases $\nu(t)$ determined from the approved statistical data [16]. A fundamentally new approach to the study of is implies the use of fractal and multifractal analysis [17]. As shown in Refs. [10, 11], for the case of Covid-19 pandemic, the function $\nu(t)$ is multifractal with an accuracy better than 1.5%. Earlier [10, 11], we analyzed $\nu(t)$ using the mathematical model of multifractal dynamics. Here we will apply a new statistical mathematical model of fractal thermodynamics. Compared to the model of multifractal dynamics, it allows the analysis of fractal properties of more complex functions $\nu(t)$, in particular, tracing the discrete dynamics of pandemic fractal state parameters. Fundamental new results in the study of fractal properties of pandemics can be expected on this way.

The paper is organized as follows. In Section 2, we prove the multifractality of daily number of diseases $\nu(t)$ for the Covid-19 pandemic. Section 3 presents the basics of the fractal thermodynamics mathematical model. Section 4 is devoted to modelling the discrete dynamics of the fractal parameters of the state of Covid-19 pandemic in the frameworks of the fractal thermodynamics. Section 5 considers 3D histograms of Covid-19 quantum phase space, summarizes the results and outlines the prospects. As initial data, we used the data of world Covid-19 statistics [16] for the time interval from January 22, 2020 to September 21, 2022.

2. Fractal properties of the number of daily diseases $\nu(t)$ for the Covid-19 pandemic

Based on the data of world statistics on Covid-19 [16], the function $\nu(t)$ of the daily number of diseases was plotted on the time interval from 01/22/2020 to 09/21/2022 (Fig. 1). The number of diseases is expressed in thousands of persons, the time t is measured in days.

The plot has a complex structure and can be qualitatively divided into three large time intervals: T_I from January 22, 2020 to September 27, 2020 (green), T_{II} from September 27, 2020 to December 21, 2021 (blue), and T_{III} from December 21, 2021 to September 21, 2022 (red).

Let us divide the three large intervals T_I, T_{II}, and T_{III} into nine smaller intervals T_i, $i = 1, 2, ..., 9$, as shown in Table 1. The large intervals T_I, T_{II}, T_{III} are unions of small intervals T_i, namely, $T_I = T_1 \cup T_2$, $T_{II} =$ (days 1–250), $T_{II} = T_3 \cup T_4 \cup T_5 \cup T_6$ (days 250–700 (450 days)), and $T_{III} = T_7 \cup T_8 \cup T_9$ (days 700–974 (274 days)).

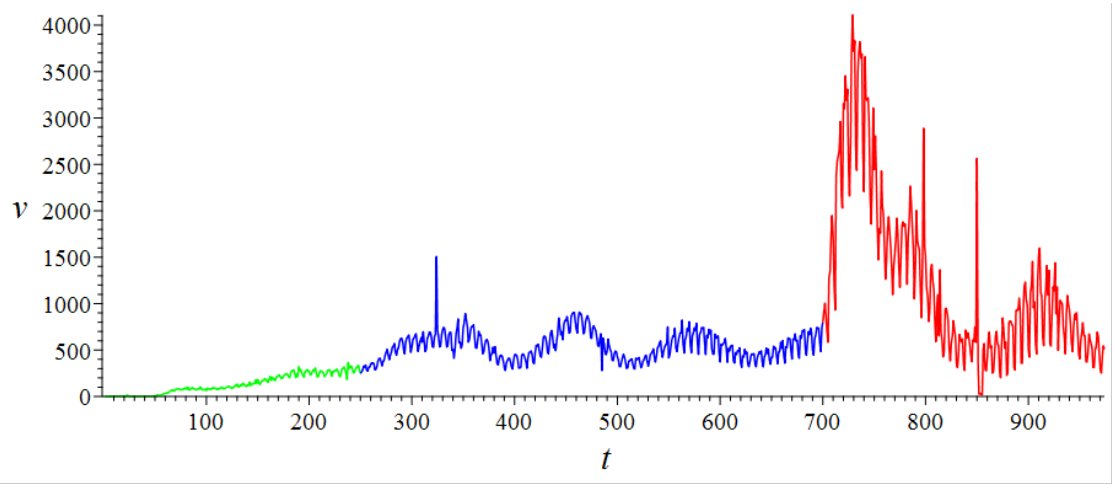

Figure 1: Plot of Covid-19 daily diseases $\nu(t)$ from 01/22/2020 to 09/21/2022, according to the world statistics [16].

Table 1: Division of time intervals.

Interval	Days	Dates	Number of days
T1	1 – 185	January 22, 2020 – July 24, 2020	185
T2	185 – 250	July 24, 2020 – September 27, 2020	65
T3	250 – 391	September 27, 2020 – February 15, 2021	141
T4	391 – 517	February 15, 2021 – June 21, 2021	126
T5	517 – 628	June 21, 2021 – October 10, 2021	111
T6	628 – 700	October 10, 2021 – December 21, 2021	72
T7	700 – 760	December 21, 2021 – February 19, 2022	60
T8	760 – 859	February 19, 2022 – May 29, 2022	99
T9	859 – 974	May 29, 2022 – September 21, 2022	115

Such a division approximately correlates with the domination of Covid-19 variants [18]:

Alpha: October 2019 to August 2020;

Beta (South African variant): June 2020 to July 2021;

Gamma (Brazilian variant): January 2021 to March 2021;

Delta (Indian variant): December 2020 to November 2021;

Omicron: December 2021 to September 2022.

Comparing these data with Fig. 1, we can associate the domination of variants Alpha and Beta with the interval T_I, Beta, Gamma, and Delta with the interval T_{II}, and Omicron with the interval T_{III}.

Let us show that function $\nu(t)$ is multifractal on the set of time intervals T_i. For this purpose, we evaluate the degree of deviation δ_i of this function from a fractal in these intervals [18, 19].

We embed the function $\nu(t)$ on the time interval T_i in the Euclidean space $\mathbf{R}^2$ and cover it with $\mathbf{R}^2$-cubes with side h. The number of cubes covering the function $\nu(t)$ on the interval T_i is denoted $N_i(h)$. We approximate the function $N_i(h)$ by the power function $\bar{N}_i(h) = \Gamma_i h^{-D_i}$. If we choose a sequence of values of h_k, $k = 1, 2, \ldots, K$, then the deviation δ_i of the functions $N_i(h)$ from $\bar{N}_i(h)$ can be estimated as

$$\delta_i = \max_{1 \le k \le K} \left| N_i(h_k) - \bar{N}_i(h_k) \right| / \bar{N}_i(h_k). \tag{1}$$

If $\delta_i = 0$, then the function $\nu(t)$ on the interval T_i is a strict fractal. In the case when $\delta_i \neq 0$, but $\delta_i \ll 1$, the function $\nu(t)$ will be considered an approximate fractal with the accuracy δ_i on the interval T_i. Then the approximation parameters D_i and Γ_i will be the fractal dimension of the function $\nu(t)$ and its D-dimensional fractal volume on the interval T_i, respectively.

To calculate the parameters D_i, Γ_i, and δ_i, we developed and implemented a software package in *Maple*. The results of calculations using this package for function $\nu(t)$ on time intervals T_i are summarized in Table 2.

Table 2: Calculated fractal parameters for function $\nu(t)$.

i	D_i	$\ln \Gamma_i$	δ_i
1	1.25833364	7.70217093	0.0203105413198
2	1.30947731	8.01320886	0.0432256670197
3	1.25731099	9.84759722	0.0088491053326
4	1.32155390	9.72026998	0.0345168719067
5	1.43820614	10.01227596	0.0269740830816
6	1.37196424	9.58254051	0.0441383504391
7	1.28275367	11.54414535	0.0408513019061
8	1.25289894	11.34705590	0.0220051023750
9	1.42855976	11.48599502	0.0498193434711

For all time intervals T_i, the value of δ_i does not exceed 5%. With this accuracy, the function $\nu(t)$ is proved to be multifractal.

3. Fractal thermodynamics

From Table 2, the multifractal character of function $\nu(t)$ follows, which stimulates applying the model of fractal thermodynamics [18,19] to its analysis. Let us briefly formulate its basic ideas and definitions. According to [21], the fractal entropy S_f of function $\nu(t)$ on each time interval T_i is defined as

$$S_{fi} = \ln \Gamma_i. \tag{2}$$

Since Γ_i is the fractal volume, it follows that the quantity S_{f_i} characterizes the state variability in a fractal system.

Along with the fractal entropy S_{fi}, we will use the fractal temperature T_{fi} [22]:

$$T_{fi} = a\left(\frac{1}{2 - D_i} - \frac{1}{2}\right). \tag{3}$$

The interpretation of the fractal temperature T_{fi} follows from Eq. (3): it is a function of the fractal dimension D_i, which characterizes the structure complexity of function $\nu(t)$ on the time interval T_i. The coefficient a in Eq. (3) for calculating the fractal temperature T_{fi} is chosen by reasons of convenience in each particular case. In the present case, the following universal normalization arises for any value of the parameter a: $T_{fi} = 0$ for $D_i = 0$. Therefore, the scaling factor of the fractal temperature will be chosen as $a = 10$. Fractal thermodynamics is aimed to study macroscopic properties of fractal systems. It is an example of a more general concept of applying the methods of tropical mathematics to problems of thermodynamics of various dynamic systems, proposed and developed by V. P. Maslov [22].

Since the fractal parameters Γ and D enter the relation $\bar{N}(h) = \Gamma h^{-D}$, there must be a functional dependence between the fractal entropy S_f and fractal temperature T_f reflecting the structure of the multifractal function $\nu(t)$. This functional dependence can be visually presented by $S_f T_f$-diagram, in which the states of a multifractal system are mapped by points with Cartesian coordinates S_{fi} and T_{fi}.

We approximate the set of $S_f T_f$-diagram points by power functions

$$S_f = A T_f^{\gamma}. \tag{4}$$

By analogy with classical thermodynamics, Eq. (8) will be referred to as the fractal equation of state (FES). Parameters γ and A, which specify the FES, will be called the FES exponent and the pre-power coefficient, respectively.

Upon approximating the set of all states S_{fi}, T_{fi} by FESs (8), the set separates into subsets, each close to a certain FES with specific parameters γ and A. Let us call each of these subsets a fractal phase state, and a transition of the multifractal system from one fractal phase state to another a fractal phase transition. The discrete dynamics of fractal phase states is characterized by jumps in parameters γ and A.

Along with S_f and T_f, it is of undoubted interest to introduce the fractal state parameter E_f , the fractal energy, defined as

$$E_f = \frac{\gamma}{1+\gamma} T_f S_f = \frac{\gamma}{1+\gamma} A T_f^{1+\gamma}. \tag{5}$$

Within the fractal thermodynamics developed here, we will consider the parameters S_f, T_f, E_f as specifying a fractal thermodynamic state. The discrete dependence of these parameters on time is the discrete dynamics of the system.

4. Discrete dynamics of Covid-19 pandemic fractal parameters

To describe the discrete dynamics of the fractal state parameters, we introduce a discrete set of time points t_i, $i = 1, 2, ..., 9$:

$$t_i = \sum_{k=1}^{i} T_f^{1+\gamma} k. \tag{6}$$

On time intervals $0 \le t \le T_1 \quad (i = 1)$, $t_{i-1} \le t \le t_i \quad (i \ge 2)$ we put $\delta(t_i) = \delta_i$, $S_f(t_i) = S_{fi}$, and $T_f(t_i) = T_{fi}$.

Using the data of Table 2, we calculated the parameters δ_i, S_{fi}, and T_{fi} from Eqs. (2) and (3) at points t_i from Eq. (6) and presented them in Table 3. Using the

Table 3: Calculated values of fractal parameters δ_i, S_{fi}, T_{fi}.

i	δ_i	S_{fi}	T_{fi}
1	0.0203105413198	7.70217093	8.48315170
2	0.0432256670197	8.01320886	9.48178342
3	0.0088491053326	9.84759722	8.46458592
4	0.0345168719067	9.72026998	9.73956434
5	0.0269740830816	10.01227596	12.80012334
6	0.0441383504391	9.58254051	10.92266028
7	0.0408513019061	11.54414535	8.94221155
8	0.0220051023750	11.34705590	8.38506995
9	0.0498193434711	11.48599502	12.49964278

data of Table 3, let us plot the functions $\delta(t)$, $S_f(t)$, $T_f(t)$ at points t_i. In the figures below, green dots correspond to time interval T_I, blue dots to T_{II}, and red dots to T_{III}. From Table 3 and Fig. 2, it is seen that the deviation of function $\nu(t)$ from a strict fractal on each of time intervals T_i satisfies the inequality $0.0088 < \delta < 0.0498$. This fact testifies for the multifractal nature of the number of daily diseases function

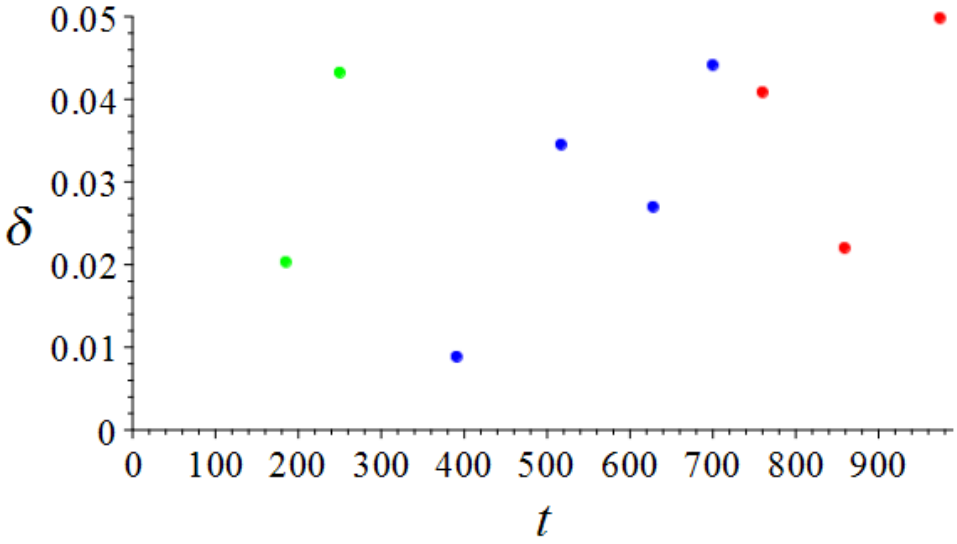

Figure 2: Discrete values of function $\delta(t_i)$.

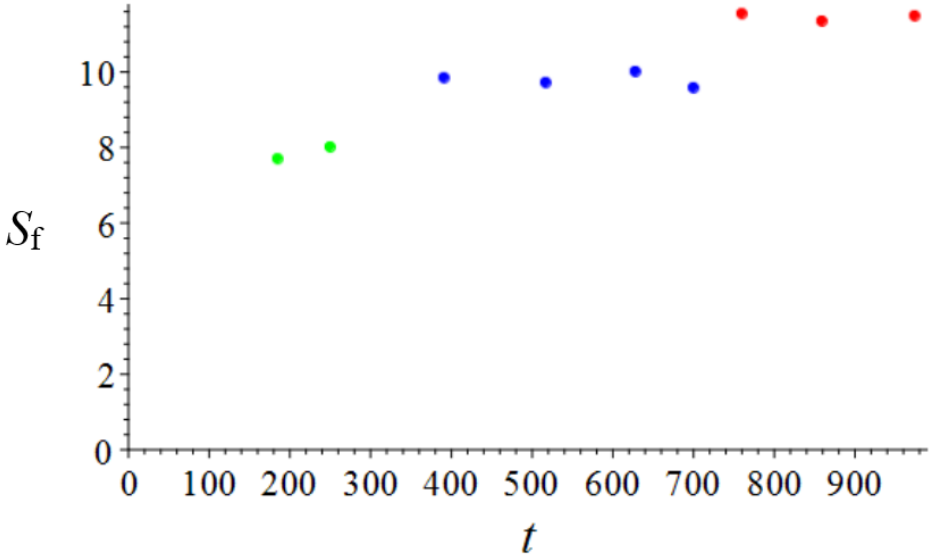

Figure 3: Discrete values of fractal entropy $S_f(t_i)$.

$\nu(t)$ during the Covid-19 pandemic period from 22/01/2020 to 21/09/2022. Fig. 3 illustrates the dependence of fractal entropy $S_f(t)$ of the number of daily diseases $\nu(t)$ within the studied time interval. From Fig. 3, we see that the function $S_f(t)$ is close to linear in three domains of the (t, S_f)-plane on each of the selected time intervals T_I, T_{II}, T_{III}.

The fractal temperature T_f as a function of time (Fig. 4) demonstrates two regions of oscillatory behavior with periods of 391 and 468 days. The oscillation amplitudes amount to 1.017 and 4.415, respectively.

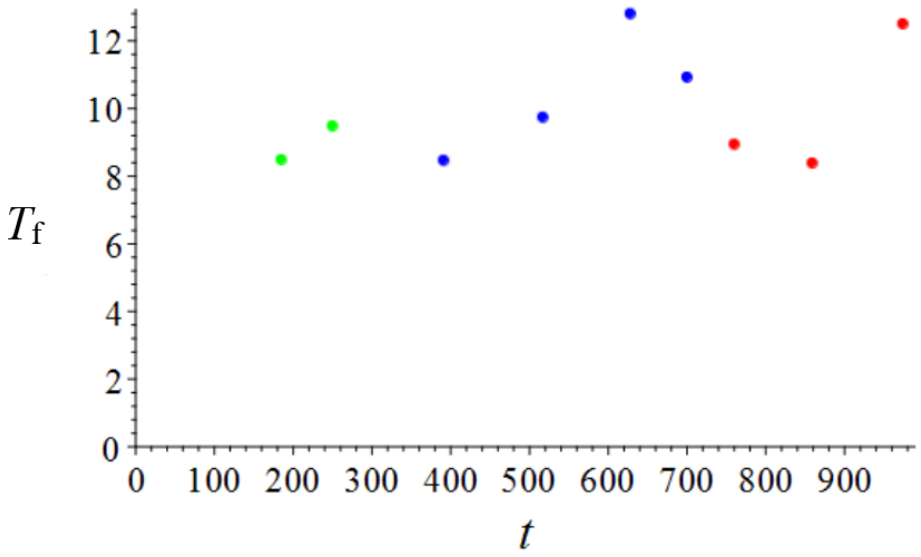

Figure 4: Discrete values of fractal temperature T_{fi}.

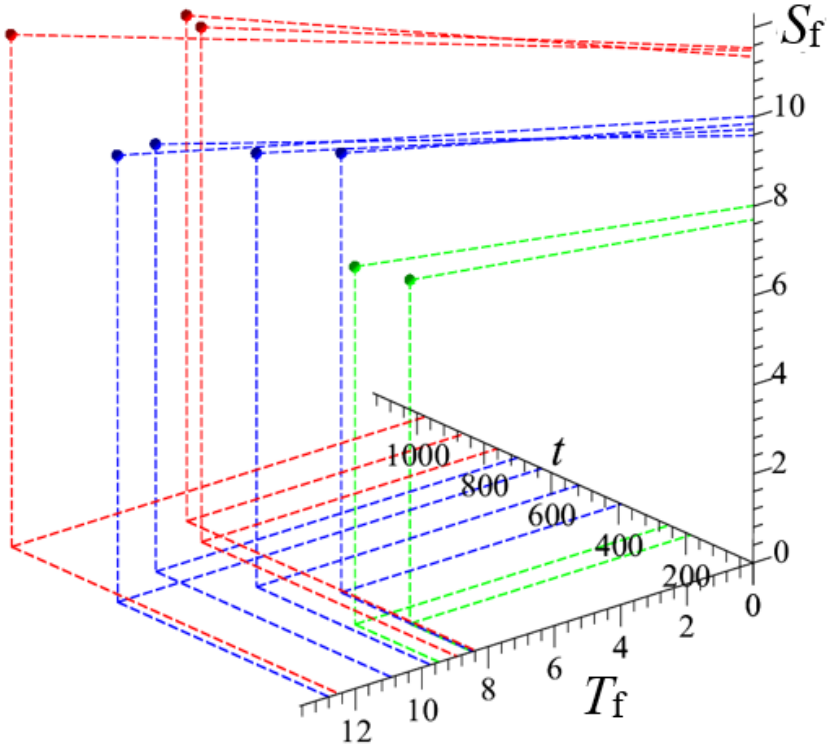

Figure 5: 3D diagram of time dependences S_{fi} and T_{fi}.

The plots of discrete functions S_{fi} and T_{fi} shown in Figs. 3 and 4 can be combined in a single discrete 3D diagram (Fig. 5). Fig. 5 shows the projections of the discrete fractal state parameters S_f and T_f on the coordinate axes, which allows presenting their discrete dynamics in a simple and visual form.

Using the data of Table 3 it is possible to construct fractal diagrams of states (FES curves) of Covid-19 pandemic in the time interval under study.

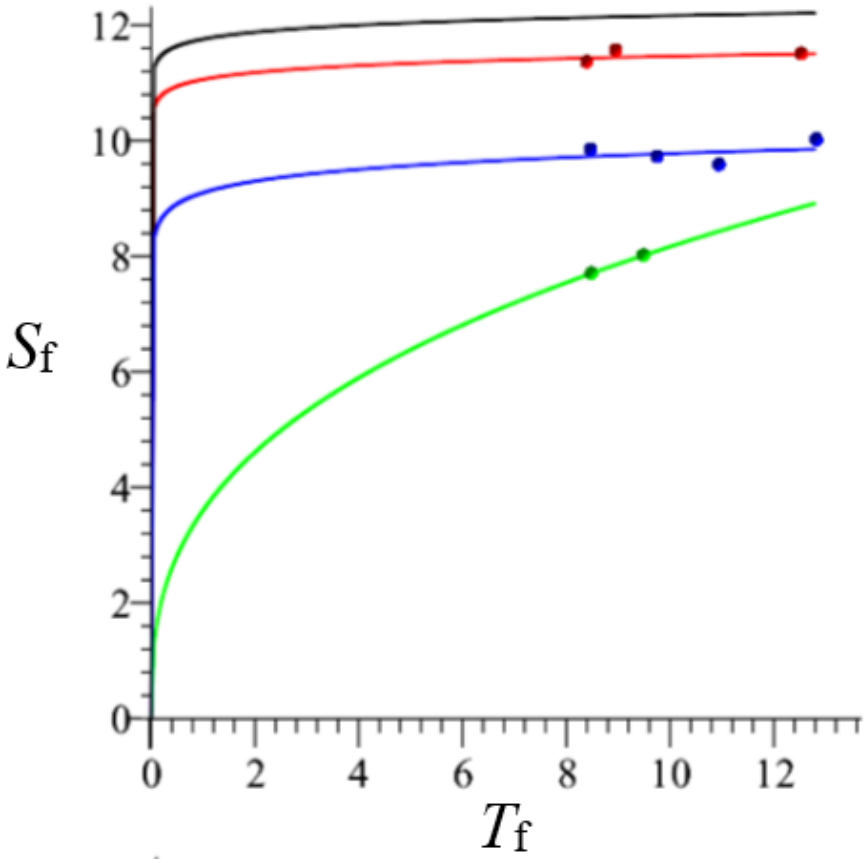

Figure 6: Discrete fractal diagrams of state (FES curves) for COVID-19 pandemic.

In Fig. 6, the green curve corresponds to the time interval T_I, blue to T_{II}, red to T_{III}, and black to the forecasted interval T_{IV}. Each of the first three curves describes the corresponding fractal phase state. In this case, three fractal phase states of the Covid-19 pandemic arise during the time from 22/01/2020 to 21/09/2022. The fourth one is forecasted.

The fitted values of FES parameters A_m, γ_m (m being the interval number), corresponding to three curves in Fig. 6, are presented in Table 4. From the data of

Table 4: FES approximating parameters A_m, γ_m.

m	A_m	γ_m
I	3.59997697725635	0.355727592986924
II	9.10162859574631	0.031155925132403
III	11.0605428390201	0.015506936570120

Table 4, a monotonic decrease in the FES exponent γ_m and increase in pre-power coefficient A_m is seen upon an increase in m. The following relations between the coefficients A_m, γ_m are observed for $m = 1$:

$$A_{m+2} = 1.356A_{m+1} - 0.356A_m, \qquad \gamma_{m+2} = 1.0482\gamma_{m+1} - 0.0482\gamma_m. \tag{7}$$

To extend A and γ over the forecasted interval T_{IV} ($m = IV$), we assume that Eq. (7) are valid for further values of m and get $A_{IV} = 11.7580$, $\gamma_{IV} = 0.01475$, based on which the black forecasted curve in Fig. 6 is drawn.

As follows from Eq. (7), the descending sequence γ_m is converging and its limit equals 0.0147. In contrast to the sequence γ_m, the sequence A_m is ascending and its limit equals 12.143. Hence, the asymptotic fractal equation of state takes the form:

$$S_f = 12.143T_f^{0.0147}. \tag{8}$$

The jumps in parameters A_m and γ_m of FES $S_f = AT_f^{\gamma}$ indicate fractal phase transitions between the fractal phase states of the Covid-19 pandemic process. The decrease in the value of A_m and γ_m jumps when proceeding from interval T_m to interval T_{m+1} indicates a decrease in the intensity of fractal phase transitions with time and stabilization of fractal phase states of the Covid-19 pandemic state.

5. 3D histograms of Covid-19 quantum phase space (QPS)

Consider the pandemic dynamics in the 2D phase space (ν, a), where, as above, ν [thousand people/day] is the number of daily diseases ('speed'), a [thousand people/day^2] is the change rate of the number of daily diseases ('acceleration'), n is the occupation number (the number of repeated pairs ν and a). The pair $(\nu(t), a(t))$ describes the phase trajectory of pandemic in the phase space. Functions $\nu(t)$, $a(t)$ (the state variables of the Covid-19 dynamics) are quantized with step h [18, 19], thus making the phase space quantized into discrete cells. In the process of motion, the phase state point occupies different cells of the phase space with different probability, which is evaluated by the occupation number (number of visits) n. Thus, the pandemic process can be presented by a state point travelling from one cell to another, while the phase trajectory as a whole can be described by the dependence of n upon (ν, a) - the 3D histogram. Both representations can be considered to illustrate the 'difference in complexity' underlying the fractal entropy. Animations of phase point motion in the QPS and 3D histograms of the phase trajectories were obtained based on the statistics of Covid-19 for the entire world, Russia, the USA, and China during the time from the pandemic beginning to 06/02/2022 (Figs. 7– 9). We use dimensionless values of ν and a. For each case we introduce a threshold value $a = a_l$, where $l = 1$ for the world, $l = 2$ for Russia, $l = 3$ for the USA, $l = 4$ for China. For clarity, the states with $|a| < a_l$ are shown in green, $a > a_l$ in red, and $a < -a_l$ in blue. Based on the statistical data, we have chosen $a_1 = 250, a_2 = 2, a_3 = 200, a4 = 0.5$.

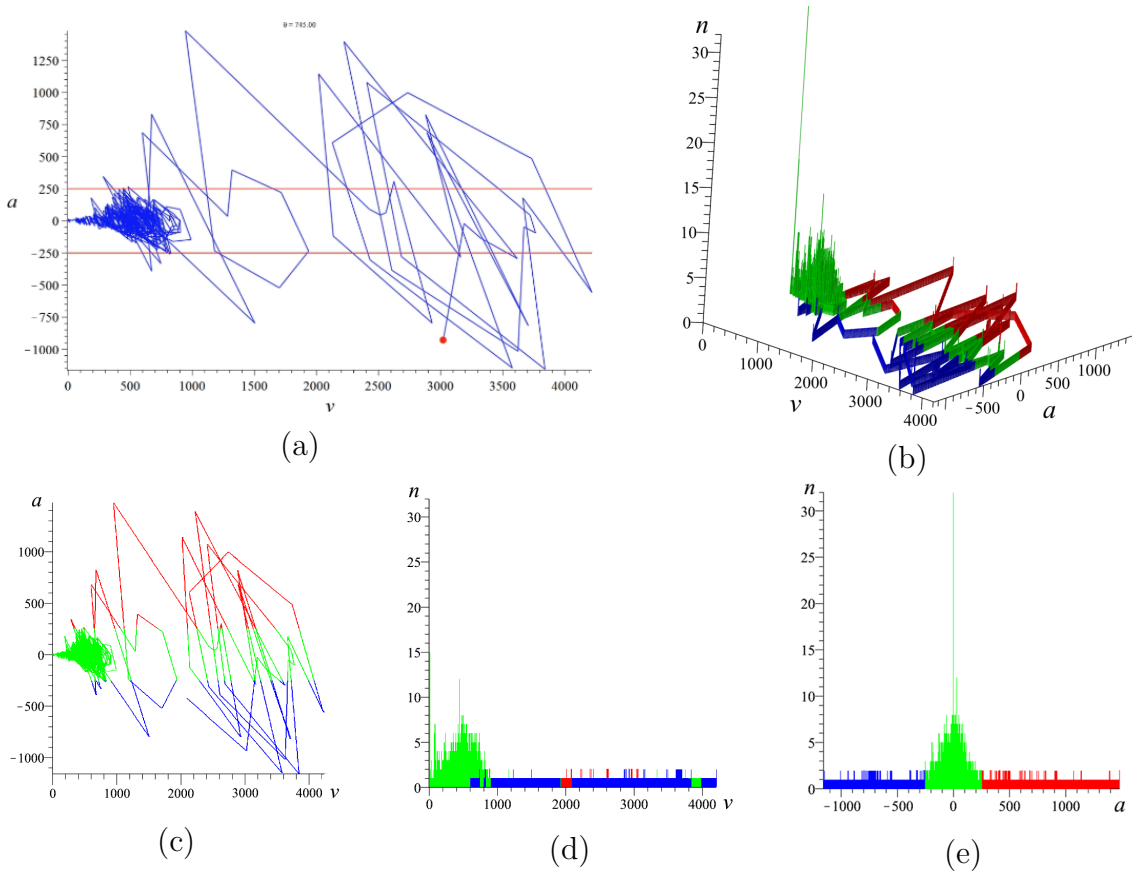

(a) (b) (c) (d) (e)

Figure 7: Animation of phase point motion (a), 3D QPS Covid-19 histogram (b) and its projections on the coordinate planes νa (c), νn (d), an (e) for the world. The quantization step $h = 5$.

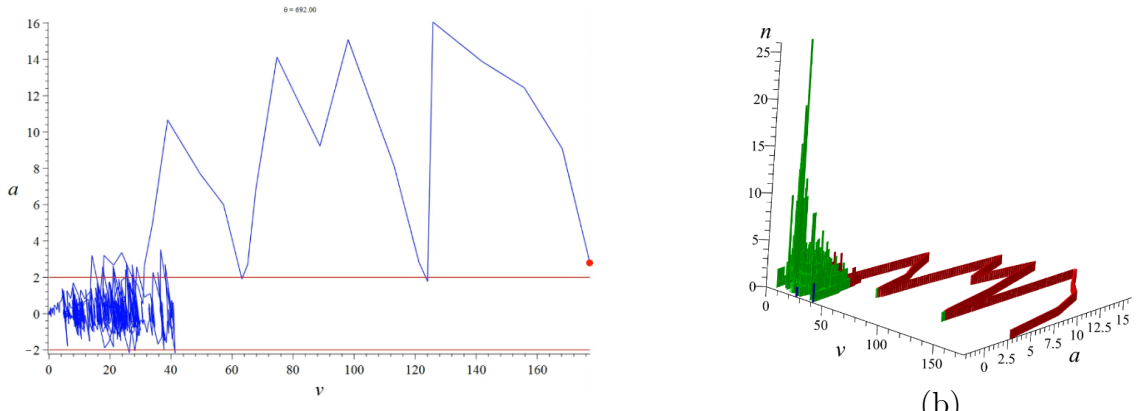

(a) (b)

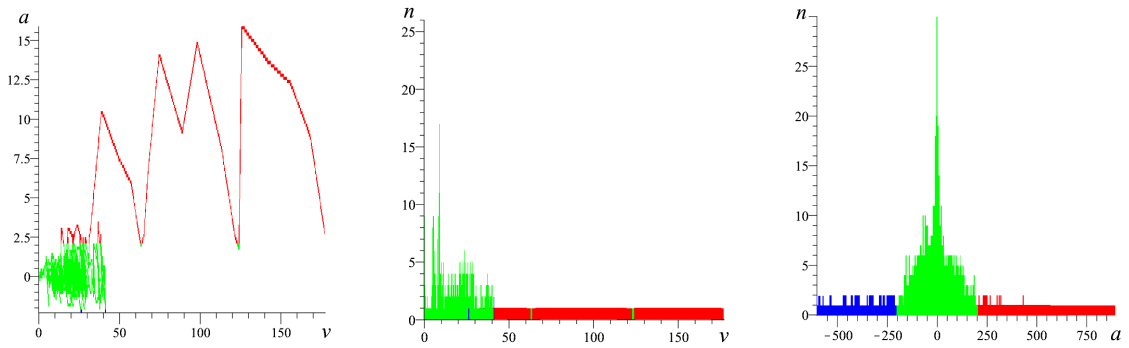

Figure 8: Animation of phase point motion (a), 3D QPS Covid-19 histogram (b) and its projections on the coordinate planes νa (c), νn (d), an (e) for Russia. The quantization step $h = 0.2$.

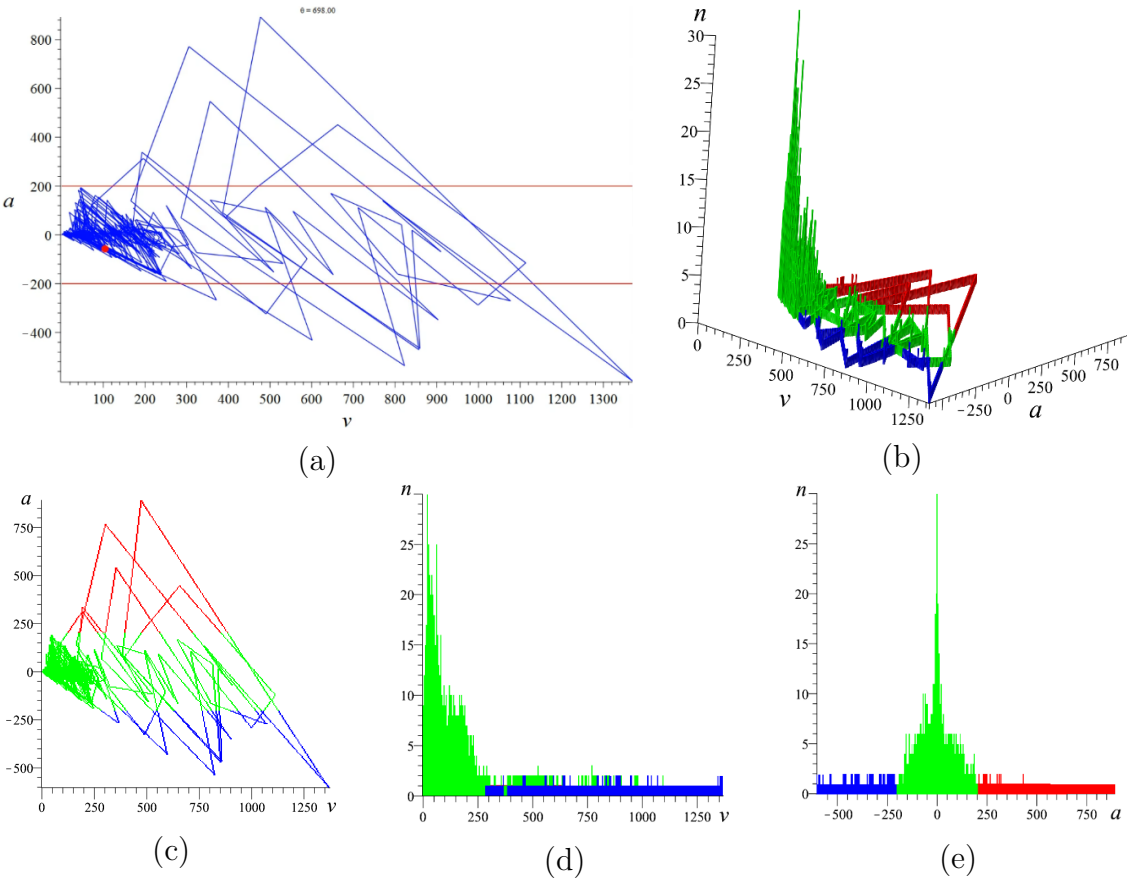

Figure 9: Animation of phase point motion (a), 3D QPS Covid-19 histogram (b) and its projections on the coordinate planes νa (c), νn (d), an (e) for the USA. The quantization step $h = 5$.

Figs. 7b– 10b demonstrate compact regions of the phase trajectory thickening, inside which the phase point stays much longer than in other regions. These areas play the role of attractors in the Covid-19 quantum phase space.

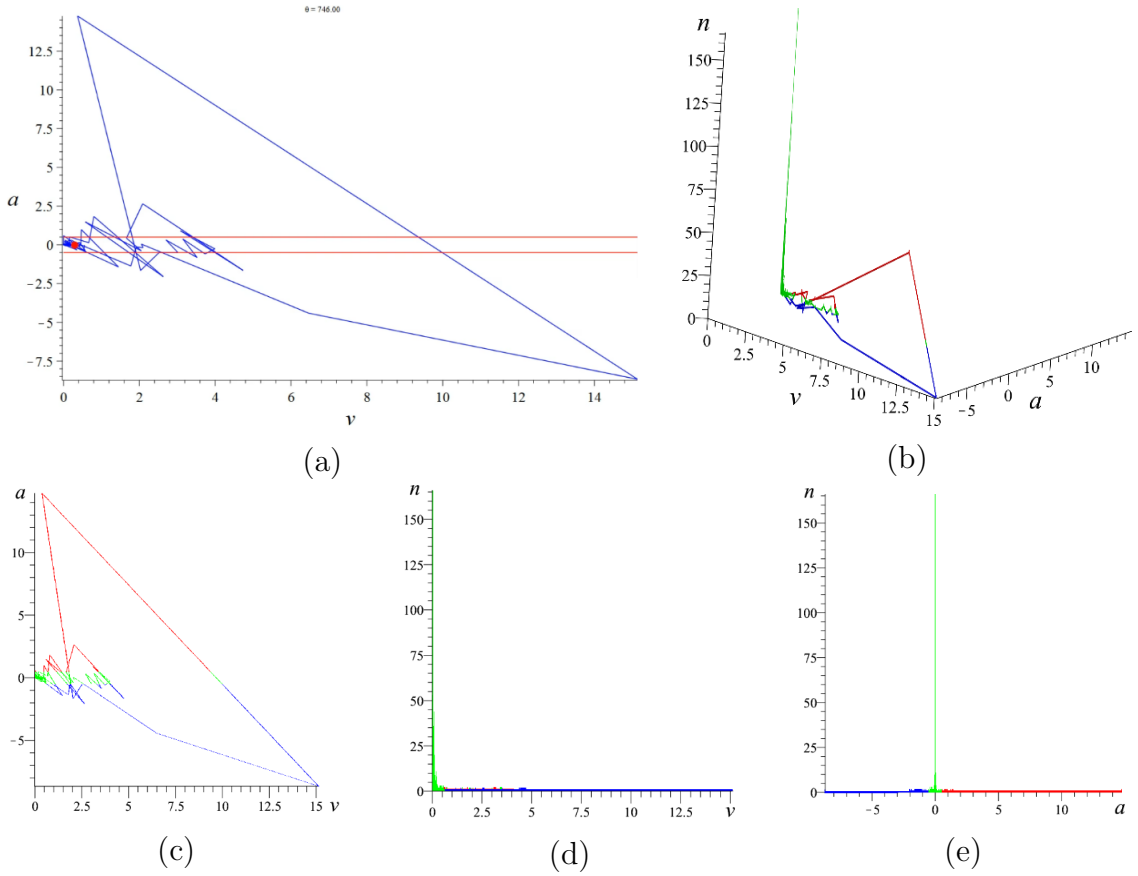

Figure 10: Animation of phase point motion (a), 3D QPS Covid-19 histogram (b) and its projections on the coordinate planes νa (c), νn (d), an (e) for China. The quantization step $h = 0.1$.

Table 5: Covid-19 QPS Fractal dimension D_l and fractal entropy S_l for the world and selected countries.

l	*Country*	D_l	S_l
1	World	1.1842	11.4124
2	Russia	1.2191	5.8252
3	USA	1.2384	10.5161
4	China	1.0422	4.3880

We also calculated the values of fractal dimension D_l and fractal entropy S_l in the QPS of Covid-19 for the countries considered (see Table 5). In spite of close

values of the fractal dimension for all cases, the values of fractal entropy strongly differ between the pair world – USA, on the one hand, and the pair Russia – China, on the other hand. Visible correlation of this observation with the difference in the phase point behavior and 3D histograms again testifies for the reasonability of fractal thermodynamic approach.

6. Conclusion

Based on the Covid-19 world statistical data, three-time intervals are distinguished, qualitatively differing by the structure of function $\nu(t)$ describing the daily number of diseases. These time intervals are shown to correlate with the domination of particular variants of Covid virus. Earlier, using the standard technique of fractal analysis implemented by us in a Maple software package, we approved the multifractality of function $\nu(t)$ with accuracy not worse than 5% in the time interval considered. In this paper, we develop the fractal approach to characterize the Covid-19 pandemic macroscopically by using the fractal thermodynamics model. Within this model, we calculated the fractal entropy $S_f(t)$ and fractal temperature $T_f(t)$ at discrete time points ti (Table 3), which determine the discrete temporal behavior of the fractal parameters of state of Covid-19 pandemic, clearly visualized in Figs. 3– 5. Based on the data of Table 3, we plotted in Figs. 6 discrete fractal diagrams of state and three FES curves for the Covid-19 pandemic on the time interval considered. Each of the curves corresponds to a fractal phase state of Covid-19 pandemic. The FES approximation parameters A_m and γ_m (m being the interval number) are summarized in Table 4, from which it follows that the FES exponent γ_m monotonically decreases and the pre-power coefficient A_m increases upon proceeding from the previous time interval T_m to the next one. Sequential values of the approximation parameters A_m and γ_m are found to satisfy recurrence relations Eq. (7), continuing which over the forecast interval T_{IV} ($m = IV$) we find the predicted parameters $A_{IV} = 11.7580$, $\gamma_{IV} = 0.01475$ used to draw the forecast curve in Fig. 6.

In the limit $m \to \infty$, we find the asymptotic fractal equation Eq. (8) of state $S_f = 12.143 T_f^{0.0147}$.

The jumps in the FES fractal parameters A_m and γ_m can be interpreted as fractal phase transitions between fractal phase states of the Covid-19 pandemic process. For practical purposes, it is possible to use the FES index, which corresponds to a certain state of the system, each state having its own curve in Fig. 6. Each curve corresponds to the disease incidence in the period, when a certain variant of Covid-19 dominated. The phase transition indicates the beginning of the dominance of a new strain. A decrease in the jumps of the parameters A_m and γ_m upon proceeding from T_m to T_{m+1} indicates a decrease in the intensity of fractal phase transitions with time and stabilization of fractal phase states of the Covid-19 pandemic process.

Animations of phase point motion in the quantum phase space (QPS) and 3D histograms of the phase trajectories were obtained based on the official statistics of Covid-19 for the world, Russia, the USA, and China from beginning of the pandemic to 06/02/2022 (Figs. 7– 10) and the corresponding values of fractal dimension D_l and fractal entropy S_l in the QPS of Covid-19 were also calculated and shown in Table 5. One can see that in spite of close values of the fractal dimension for all cases, the values of fractal entropy strongly differ between the pairs world – USA and Russia – China, correlating with the apparent difference in the phase point behavior and 3D histograms, which again testifies for the reasonability of fractal thermodynamic approach.

Thus, the characteristic features of the discrete dynamics of the fractal thermodynamic state parameters of the Covid-19 pandemic from 01/22/2020 to 09/21/2022 are revealed. It is shown that these features can be used to predict the discrete dynamics of pandemics and other similar processes.

7. Authors' contributions

The authors declare that the study was realized in collaboration with the same responsibility. All authors read and approved the final manuscript.

8. Declaration of Competing Interest

The authors declare that they have no known competing financial interests or personal relationships that could have appeared to influence the work in this paper.

9. Acknowledgements

The authors express their deep gratitude to V.P. Maslov for his support both in the development of the theoretical foundations of the fractal thermodynamics model and in its application to the study of fractal properties of specific dynamical system.

The work was partially supported by the RUDN University Strategic Academic Leadership Program, project No. 021934-0-000.

References

[1] Barzon J., Manjunatha K.K.H., Rugel W., Orlandini E., and Baiesi M. Modelling the deceleration of COVID-19 spreading. J. Phys. A: Math. Theor. 2021; 54, 044002-1-12. doi: 10.1088/1751-8121/abd59e

[2] Derbov V.L., Vinitsky S.I., Gusev A.A., Krassovitskiy P.M., Pen'kov F.M. Chuluunbaatar G. Mathematical model of COVID-19 pandemic based on a retarded differential equation. Proc. SPIE. 2021; 11847. 1184709-1-15. doi: 10.1117/12.2589136

[3] Vinitsky S.I., Gusev A.A., Derbov V.L., Krassovitskiy P.M., Pen'kov F.M. Chuluunbaatar G. Reduced SIR model of COVID-19 pandemic. Comput. Math. Math. Phys. 2021; 61(3):376–87. doi: 10.1134/S0965542521030155

[4] Pen'kov F.M., Derbov V.L., Chuluunbaatar G., Gusev A.A., Vinitsky S. I., Gozdz M., and Krassovitskiy P. M. Approximate Solutions of the RSIR Model of COVID-19 Pandemic. A. Byrski et al. (Eds.): ANTICOVID 2021, IFIP AICT 2021; 616: 53–64. doi: 10.1007/978-3-030-86582-5-6

[5] A. Gowrisankar, T.M.C. Priyanka, S. Banerjee, Omicron: a mysterious variant of concern. Eur. Phys. J. Plus 137(1), 1–8 (2022).

[6] Păcurar Cristina-Maria, Necula Bogdan-Radu . An analysis of COVID-19 spread based on fractal interpolation and fractal dimension. Chaos, Solitons and Fractals . 2020; 139:110073. refhub.elsevier.com

[7] Agrawal Ekta and Verma Saurabh. Dimensional study of COVID-19 via fractal functions. Eur. Phys. J. Spec. Top. doi: 10.1140/epjs/s11734-023-00774-z

[8] C. Kavitha, A. Gowrisankar, S. Banerjee. The second and third waves in India: when will the pandemic be culminated? Eur. Phys. J. Plus 136(5), 1–12 (2021)

[9] Easwaramoorthy D., Gowrisankar A., Manimaran A., Nandhini S., Rondoni Lamberto, Banerjee Santo. An exploration of fractal-based prognostic model and comparative analysis for second wave of COVID-19 diffusion. Nonlinear Dyn. 2021; 106:1375–1395. doi: 10.1007/s11071-021-06865-7

[10] Tsvetkov V.P., Mikheev S.A., Tsvetkov I.V., Derbov V.L., Gusev A.A., Vinitsky S.I. Modeling the multifractal dynamics of Covid-19 pandemic .Chaos, Solitons and Fractals. 2022. 161:112301. doi: 10.1016/j.chaos.2022.112301

[11] Derbov V.L., Gusev A.A., Vinitsky S.I., Mikheev S.A., Tsvetkov I.V., Tsvetkov V.P. Modeling the multifractal dynamics of Covid-19 pandemic // Progress in Biomedical Optics and Imaging. Proceedings of SPIE. 2022; 12194: SPIE, art.no.121940H.

[12] Hasib Khan, Farooq Ahmad, Osman Tunc, Muhammad Idrees. On fractal-fractional Covid-19 mathematical model. Chaos, Solitons and Fractals 2022. 157:111937. doi: 10.1016/j.chaos.2022.111937

[13] Astinchap B., Ghanbaripour H., Amuzgar R. Multifractal analysis of chest CT images of patients with the 2019 novel coronavirus disease (COVID-19). Chaos Solitons and Fractals. 2022; 156: 111820. doi: 10.1016/j.chaos.2022.111820

[14] Sokolov A.V., Sokolova L.A. COVID-19 dynamic model: balanced identification of general biological and country specific features. Procedia Comput. Sci. 2020;178: 301–10. creativecommons.org

[15] Xueyong Zhou, Yaozong Deng. Dynamic analysis of a fractional-order delayed SIQR epidemic model for COVID-19 pandemic. Mathematical Modelling and Geometry 2023; V. 11, No 3, pp. 1–20.

[16] Covid-19 World Statistics. Covid.observer

[17] Lopes R., Betrouni N. Fractal and multifractal analysis: A review. Medical Image Analysis 2009; 13: 634–49. doi: 10.1016/j.media.2009.05.003

[18] Variants of SARS-CoV-2. en.wikipedia.org/wiki

[19] S.A. Mikheev, E.K. Paramonova, V.P. Tsvetkov, I.V. Tsvetkov Fractal Thermodynamics of the States of Instantaneous Heart Rhythm. Russian Journal of Mathematical Physics. 2021; 28: 251–256.

[20] E.K. Paramonova, A.N. Kudinov, S.A. Mikheev, V.P. Tsvetkov, I.V. Tsvetkov. Fractal Thermodynamics, Big Data and its 3D Visualization, Proceedings of the 9th International Conference "Distributed Computing and Grid Technologies in Science and Education" (GRID'2021), Dubna, Russia, July 5–9, 2021.

[21] Tsvetkov V.P., Mikheyev S.A., Tsvetkov I.V. Fractal phase space and fractal entropy of instantaneous cardiac rhythm. Chaos, Solitons and Fractals. 2018. 108: 71–76. doi: 10.1016/j.chaos.2018.01.030

[22] Kudinov A.N., Tsvetkov V.P., Tsvetkov I.V. Catastrophes in the multi-fractal dynamics of social-economic systems. Russ J Math Phys. 2011; 18(2):149–55. doi: 10.1134/S1061920811020038

[23] Maslov V. P. Thermodynamics, Idempotent Analysis, and Tropical Geometry as a Return to Primitivism. Russ. J. Math. Phys. 2016. 23(2) : 278–280. doi: 10.1134/S1061920816020126